JOURNAL OF MATERIALS SCIENCE **36** (2001) 2679–2689

A characterisation of thick film resistors for strain gauge applications

MARKO HROVAT
Jožef Stefan Institute, Jamova 39, 1000 Ljubljana, Slovenia
E-mail: marko.hrovat@ijs.si

DARKO BELAVIČ
HIPOT, Trubarjeva 7, 8310 Šentjernej, Slovenia

ZORAN SAMARDŽIJA, JANEZ HOLC
Jožef Stefan Institute, Jamova 39, 1000 Ljubljana, Slovenia

Some commercial thick film resistors with sheet resistivities from 1 kohm/sq. up to 1 Mohm/sq. were evaluated for strain gauge applications. Temperature coefficients of resistivity, noise indices and gauge factors (GFs) were measured. For the same resistor series GFs and noise indices increase with increasing sheet resistivity. However, both GFs and noise indices are different for resistors with the same nominal sheet resistivity but from different resistor series. The results indicated that the microstructure rather than the different chemical composition of the conductive phase in thick film resistors is the primary reason for the different gauge factors.

1. Introduction

The resistance of a resistor changes under an applied stress. This change of resistance is partly due to deformation i.e. the changes of dimensions of the resistor, and partly to the alteration in the specific resistivity as a result of changes in the microstructure of the material [1, 2]. The resistance of the resistor is:

$$R = \rho^* l/(w^* t) \tag{1}$$

R = resistance (ohm), ρ = specific resistivity (ohm m), l = resistor length (m), w = resistor width (m), t = resistor thickness (m).

The change of resistance under stress is shown in Equation 2, where the first term, related to the changes in specific resistivity, is due to the microstructural changes and all the other terms are due to the changes in the dimensions:

$$\mathrm{d}R/R = \mathrm{d}\rho/\rho + \mathrm{d}l/l - \mathrm{d}w/w - \mathrm{d}t/t \tag{2}$$

and:

$$\mathrm{d}A/A = \mathrm{d}(w^* t)/(w^* t) = -2^* v^* \varepsilon \tag{3}$$

$\varepsilon = \Delta l/l$ = strain, v = Poisson ratio, A = cross-sectional area (m^2).

The change of resistance is given by Equation 4, where the first part represents the resistance change due to geometrical changes and second part to those due to microstructural changes:

$$\mathrm{d}R/R = \mathrm{d}\rho/\rho + \varepsilon(1 + 2v) \tag{4}$$

The gauge factor (GF) of a resistor is defined as the ratio of the relative change in resistance and the strain:

$$\mathrm{GF} = (\Delta R/R)/\varepsilon \tag{5}$$

Geometrical factors alone result in gauge factors of 2–2.5. Gauge factors higher than this are due to microstructural changes i.e. alterations of the specific conductivity.

Thick film resistor pastes consist basically of a conducting phase, a lead borosilicate based glass phase and an organic vehicle, which burns out during high temperature processing. In most contemporary resistor compositions the conductive phase is either RuO_2 or ruthenates, mainly bismuth or sometimes lead ruthenates. Some other oxides are normally included as minor additives either as temperature coefficient of resistivity (TCR) modifiers or modifiers of the temperature coefficient of the expansion of the glass phase. The ratio between conductive and glass phases roughly determines the specific resistivity of the resistor. Thick film resistors are screen printed and fired on insulating, mainly alumina substrates. All phases of the resistor material, e.g. conductive oxides, glass phase and added modifier oxides, react with each other and also with the substrate. During firing, the resistors are a relatively short time (typically 10 min) at the highest temperature (typically 850°C). Because of this, reactions between constituents of the resistor material do not reach equilibrium so that the characteristics of the fired materials are, in a way, a compromise as a consequence of this frozen unequilibrium. The main requirements for thick film resistors are long term stability, relatively narrow tolerances of sheet resistivities after firing, a low noise

index, and a low temperature coefficient of resistivity (TCR). Most contemporary thick film resistors have TCR below 100×10^{-6}/K.

The gauge factors of thick film resistors are mostly between 3 and 15. They are higher than those of thin metal films or foils (GF 2 to 3, low TCR below 10×10^{-6}/K) and lower than those of semiconductors with gauge factors of 50 or more and high TCRs over 1000×10^{-6}/K. Some authors have also reported the development of thick film resistor materials with higher gauge factors of 40 or more [3]. However, Prudenziati *et al*. explained these very high gauge factors as being due to the micro cracks in the fired resistors [4]. Discontinuous (very thin) metal films have even higher gauge factors, from 100 up to several hundred, however, they have high TCRs and very poor long term stability [5, 6] and are therefore, at least for now, not feasible for sensor applications. Due to their stability and relatively low cost, strain gauges realised in thick film technology offer advantages in some applications over both metal film (low GF, low TCR) and semiconducting elements (high GF, high TCR) [2, 7, 8].

The gauge factors of thick film resistors increase with increasing sheet resistivity. Gauge factors of thick film resistors based on ruthenates ($Bi_2Ru_2O_7$ or $Pb_2Ru_2O_{6.5}$) are reported to be usually higher than those of resistors based on RuO_2 [5, 9, 10]. However, some results indicate that the values of the gauge factors of thick film resistors depend not only on the composition of the conductive phase but to a greater extent on the microstructure of the material [11].

Longitudinal gauge factors (GFl) of thick film resistors, formed on the thick (considerably thicker than the resistor layer) substrate are always higher than transverse gauge factors (GFt). This is schematically shown in Fig. 1. A thick film resistor is printed and fired on a ceramic substrate. If the substrate is bent, i.e. deflected, the dimensions of the resistor are changed. The resistor length increases and the resistor thickness decreases. However, in the first approximation the width of the film resistor, which is sintered on the surface of a significantly thicker substrate (typical thickness of a thick film resistor after firing is between 10 and 20 um and that of an alumina substrate 625 um), remains the same (Fig. 1a). Regardless of the direction of measurement, i.e. whether longitudinal (current parallel to the strain; Fig. 1b, left) or transversal (current perpendicular to the strain; Fig. 1b, right), the resistance of the resistor increases due to the increase in specific resistivity and the decrease in thickness. When the measurement is in a direction parallel to the strain the resistance additionally increases due to the increase of the resistor length, while in the case of the perpendicular measurement the resistance decreases by the same amount due to the increase of the resistor width. Transverse gauge factors are typically around 70% of longitudinal gauge factors [8].

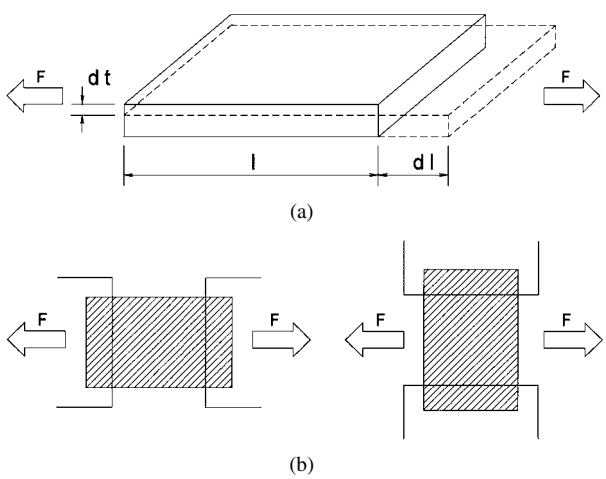

Figure 1 (a) A thick film resistor on a substrate (schematically). If the substrate is deflected, the resistor length increases and the resistor thickness decreases. In the first approximation the width of the film resistor, which is sintered on the on the surface of a significantly thicker substrate, remains the same. (b) Longitudinal measurement of resistance—current parallel to the strain (left) and transversal measurement of resistance—current perpendicular to the strain (right).

The Du Pont HS-80, QM-80, QM-90 and 2000 thick film resistor series were evaluated for strain gauge applications. Electro Science Labs. 3414 and Heraeus 8241, both with sheet resistivities of 10 kohm/sq., were also tested. The conductive phase in the resistors was determined by X-ray powder diffraction analysis and EDS (Energy Dispersive X-ray Microanalysis). Resistors from the Du Pont series HS-80 × 1 and HS-80 × 9 are based on RuO_2 (e.g. 8031, 1 kohm/sq.) or ruthenate (e.g. 8029, 1 kohm/sq.), respectively [12–14]. Electro Science Labs. 3414 paste, which was specially formulated for high gauge factors [15], is based on ruthenate and Heraeus 8241 on RuO_2. The QM-80, QM-90 and 2000 series are based on a mixture of RuO_2 and ruthenate. EDS quantitative analysis showed the presence of bismuth in HS-80 × 9, QM-80 and QM-90 materials, which indicates that the ruthenate phase in these resistors is presumably $Bi_2Ru_2O_7$. As no bismuth was detected in the 2000 series resistors, the ruthenate phase in this resistor series is assumed to be lead ruthenate, i.e. $Pb_2Ru_2O_{6.5}$.

2. Experimental

The changes of resistivity as a function of substrate deformation were measured with the simple device presented in Fig. 2. The ceramic substrate is supported on both sides. The load is applied to the middle of the substrate with a micrometer and this induces a tensile strain in the resistor. The magnitude of the strain is given by the Equation 6 [16]:

$$\varepsilon = \Delta l / l = (d * t * 6)/L^2 \qquad (6)$$

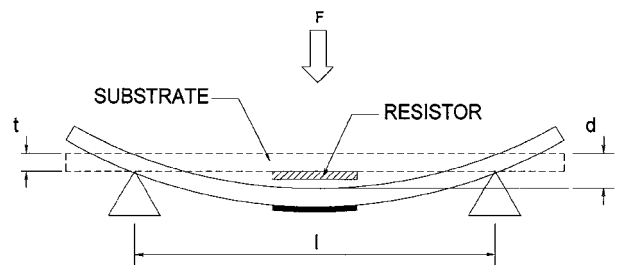

Figure 2 A method for measuring the changes of resistivity as a function of substrate deformation (schematically). The ceramic substrate is supported on both sides. The load is applied in the middle of the substrate with a micrometer and induces a tensile strain in the resistor.

d = deflection (m), t = substrate thickness (m), L = distance between support edges (m).

The gauge factors are calculated using Equation 5 from the strain and resistivity changes. For the experimental set-up shown in Fig. 2, the distance between the edge supports is 40 mm and the nominal thickness of the alumina substrates is 0.635 mm. As an example; if the resistance change is 0.25% with a deflection of 100 um, the calculated value of the gauge factor is 10.5.

Thick film resistors with dimensions 1.6×1.6 mm^2. were printed and fired at 850°C on 50×7 mm^2 96% alumina substrates. Resistors were terminated with a prefired Pd/Ag conductor for either longitudinal or transverse measurement of the resistivity changes due to the deflection of the substrates (see Fig. 1). Sheet resistivities as a function of temperature were measured. Cold (from −25°C to 25°C) and hot (from 25°C to 125°C) TCRs were calculated from resistivity measurements at −25°C, 25°C, and 125°C. Current noise was measured in dB on 100 mW loaded resistors by the Quan Tech method (Quan Tech Model 315-C).

For microstructural investigation the resistors, printed and fired on alumina ceramics, were mounted in epoxy in cross-sectional orientation and then cut and polished using standard metallographic techniques. A JEOL JSM 5800 scanning electron microscope (SEM) equipped with an energy dispersive X-ray analyser (EDS) was used for overall microstructural and compositional analysis. Prior to analysis in the SEM, the samples were coated with carbon to provide electrical conductivity and to avoid charging effects. The conductive phase in the resistors was determined by X-ray powder diffraction analysis (XRD) with a Philips PW 1710 X-ray diffractometer using Cu K_α radiation. X-ray spectra were measured from $2\Theta = 20^\circ$ to $2\Theta = 70^\circ$ in steps of 0.02°. Dimensions of resistors for microstructural analysis and X-ray diffraction analysis, which were printed and fired without conductor terminations, were 12.5×12.5 mm^2.

3. Results and discussion

Some data on the conductive phase and the quantitative results of EDS microanalysis of glass composition of thick film resistors are summarised in Table I. 10 kohm/sq. resistors are presented as typical examples. The EDS spectra of the glass phase of thick film resistors are shown in Fig. 3a (8039), b (8041), c (2041), d (QM-84), e (QM-94), f (3414) and g (8241). All glasses contain lead, silicon and aluminium oxides. Boron oxide, which is also present in the glass phase, can not be detected in EDS spectra because of the low relative boron weight fraction in glass and strong absorption of the boron K_α line during EDS analysis in the glass matrix. However, most thick film resistors use glasses with roughly equal proportions of PbO, SiO_2 and $B2O_3$, as glasses rich on PbO, SiO_2 or $B2O_3$ have high temperature expansion coefficients, high melting temperature or glass immiscibility, respectively [17].

Note that the ratio of peak intensities of the main elements varies significantly. The heights of peaks of Si and Pb are comparable for all resistors with the exception of 8241 glass, where the Pb peak is significantly stronger. Also, the height of the Al peak differs. Al_2O_3 is present only as a minor compound in Electro Science Labs. 3414 resistor. However, the relatively strong peak of alkaline element. i.e. potassium was observed in the glass phase in this resistor.

Nominal sheet resistivities, cold and hot TCRs, and noise indices are shown in Table. II. The dependence of relative resistivity vs. temperature is presented in Fig. 4a (1 kohm/sq.), b (10 kohm/sq.), c (100 kohm/sq.) and d (1 Mohm/sq.). Noise indices of the resistors are graphically presented in Fig. 5. However, note that in Fig. 5, the noise indices are expressed in "uV/V" while in Table I. They are given as "dB". These two units are related with a simple equation:

$$\text{noise (dB)} = 20 \times \log \text{noise (uV/V)} \qquad (7)$$

The TCRs of the resistors are below 100×10^{-6}/K, with the exception of QM-83 and QM-93 (hot TCR) and 3414 (cold TCR). Noise indices of resistors from the same series increase with increasing sheet resistivity. Note, however, that the noise index of the 8059 resistors is very high and could not be measured as the upper range of the Quan Tech Model 315-C instrument is

TABLE I Conductive phase and summarised quantitative results of EDS microanalysis of elements detected in glass phase of 10 kohm/sq. resistors

Resistor	Conductive phase	Main elements	Other elements detected
8039	ruthenate	Si, Pb, Al	Zr
8041	RuO_2	Si, Pb, Al	Zn, Cu
2041	RuO_2 + ruthenate	Si, Pb, Al	Mg, Zn, Ca, Ba
QM-84	RuO_2 + ruthenate	Si, Pb, Al	Cu, Zr
QM-94	RuO_2 + ruthenate	Si, Pb, Al	Ca, Mn, Cu
3414 (ESL)	ruthenate	Si, Pb	Al, K
8241 (Her.)	RuO_2	Si, Pb, Al	Ca

TABLE II Nominal sheet resistivities, cold (−25°C to 25°C) and hot (25°C to 125°C) TCRs, and noise indices of the resistors

Resistor	Nominal sheet resistivity (ohm/sq.)	Cold TCR ($\times 10^{-6}$/K)	Hot TCR ($\times 10^{-6}$/K)	Noise (dB)
8029	1 k	−45	15	−22.8
8031	1 k	−55	5	−10.6
2031	1 k	5	20	−23.6
QM-83	1 k	90	160	−18.3
QM-93	1 k	75	110	−21.2
8039	10 k	−60	0	−14.2
8041	10 k	60	70	−5.5
2041	10 k	5	20	−23.6
QM-84	10 k	−5	50	−15.8
QM-94	10 k	20	75	−17.3
3414 (ESL)	10 k	−135	−40	2.0
8241 (Her.)	10 k	10	50	−7.8
8049	100 k	15	70	−1.8
2051	100 k	−20	35	−5.3
QM-85	100 k	30	75	−3.4
QM-95	100 k	35	75	−4.2
8059	1 M	−35	30	>30
2061	1 M	−50	20	5.3
QM-86	1 M	−35	35	9.0

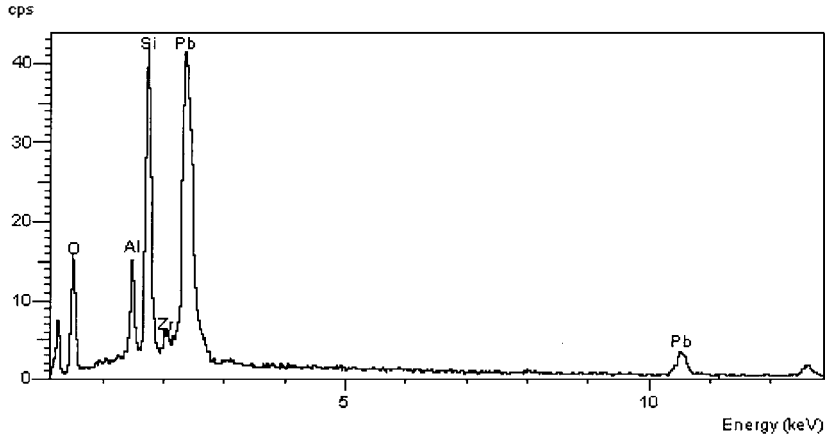

(a)

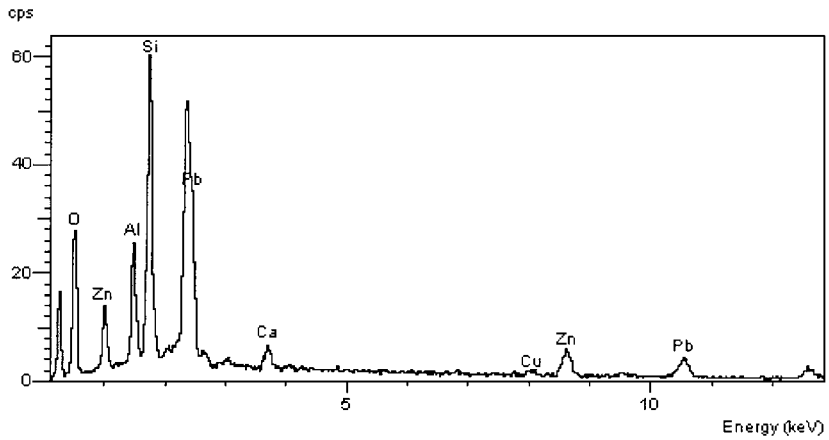

(b)

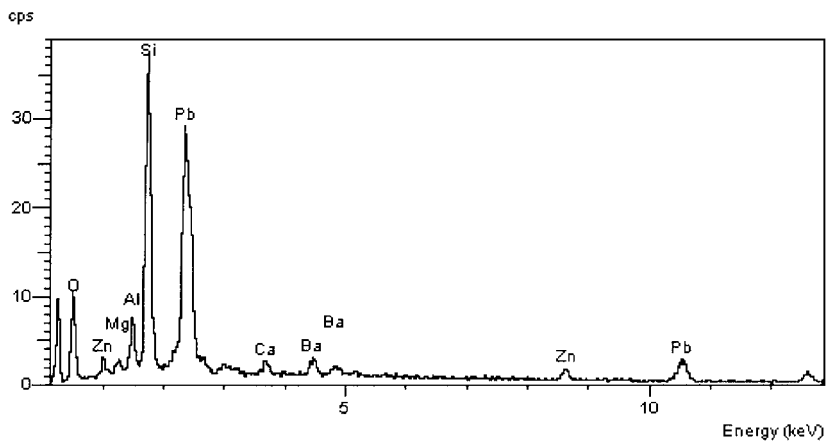

(c)

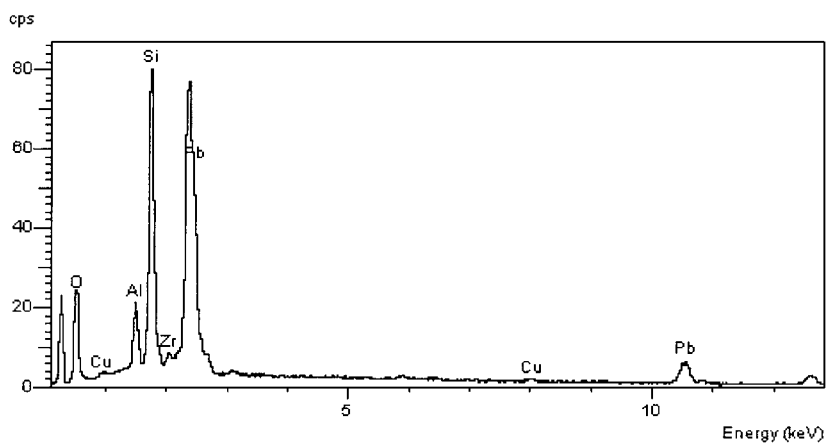

(d)

Figure 3 (a) EDS spectrum of glass phase of 8039 resistor (10 kohm/sq.), fired 10 min. at 850°C; (b) EDS spectrum of glass phase of 8041 resistor (10 kohm/sq.), fired 10 min. at 850°C; (c) EDS spectrum of glass phase of 2041 resistor (10 kohm/sq.), fired 10 min. at 850°C; (d) EDS spectrum of glass phase of QM-84 resistor (10 kohm/sq.), fired 10 min. at 850°C; (e) EDS spectrum of glass phase of QM-94 resistor (10 kohm/sq.), fired 10 min. at 850°C; (f) EDS spectrum of glass phase of 3414 resistor (10 kohm/sq.), fired 10 min. at 850°C; (g) EDS spectrum of glass phase of 8241 resistor (10 kohm/sq.), fired 10 min. at 850°C. (*Continued*.)

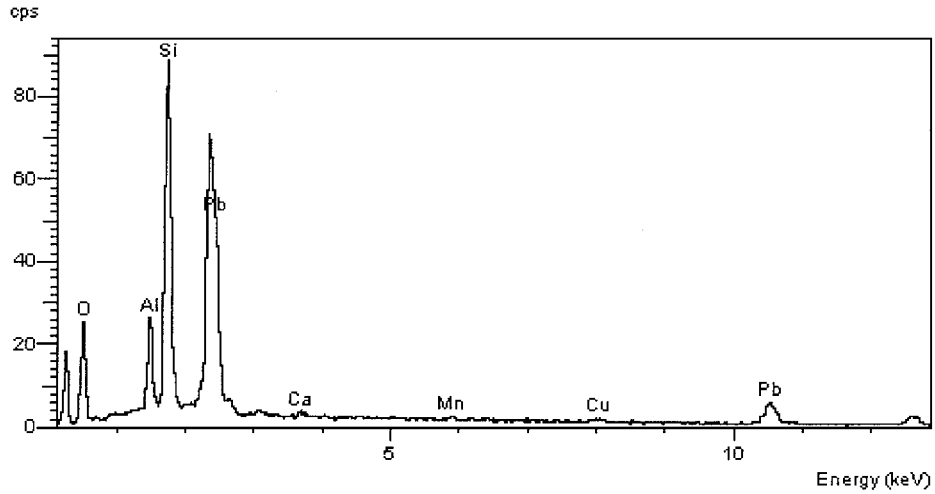

(e)

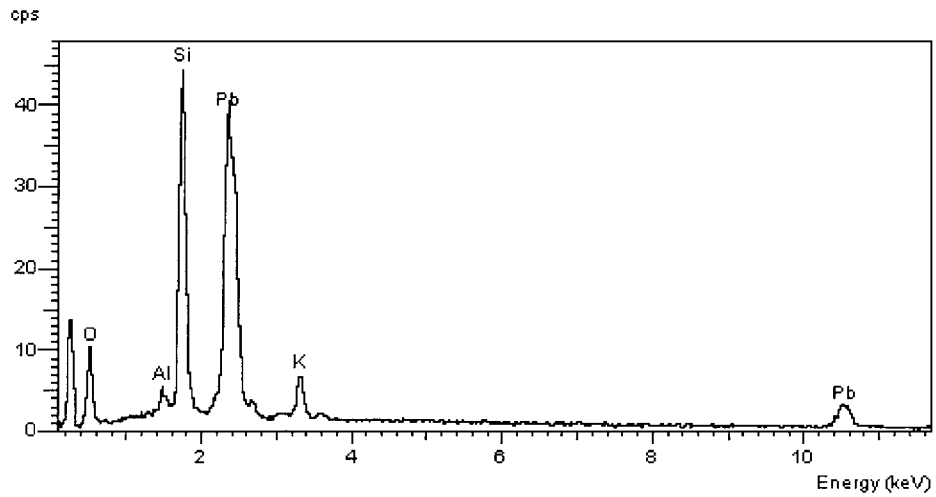

(f)

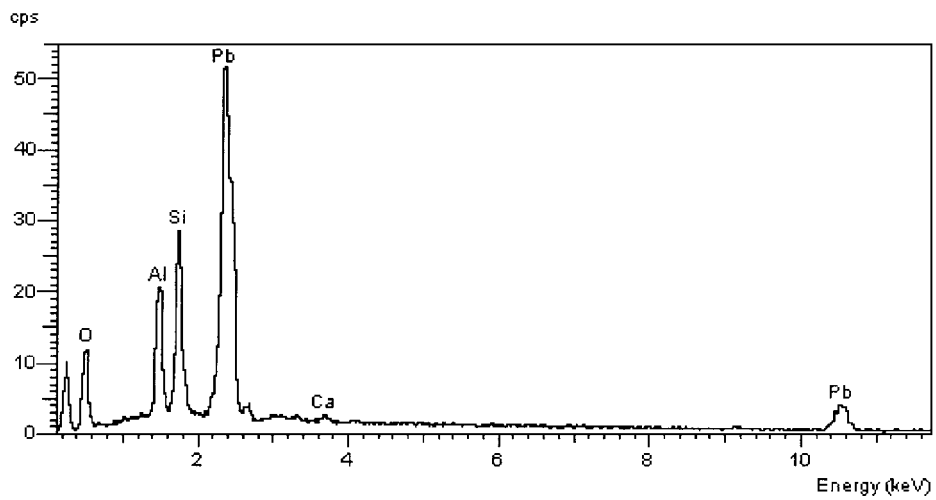

(g)

Figure 3 (*Continued.*)

+30 dB which equals 31.6 uV/V. The noise indices of the other two 1 Mohm/sq. resistors, 2061 and QM-86 are 5.3 dB (1.8 uV/V) and 9 dB (2.8 uV/V). As the scale of the noise in Fig. 3 is adjusted to 1.4 uV/V the values of the 1 Mohm/sq. resistor noise indices are cut off. With the exception of 1 Mohm/sq. resistors the ESL 3414 (10 kohm/sq) has the highest noise, around +2 dB. For comparable sheet resistivities the 2000 series has the lowest noise.

Longitudinal gauge factors (GF_l), transverse gauge factors (GF_t) and the ratio GF_t/GF_l of evaluated thick film resistors are shown in Table III. Longitudinal gauge factors (GF_l) are also graphically presented in Fig. 6. The experimental results are rounded up to 0.5, e.g. 10.0 or 10.5.

The longitudinal and transverse gauge factors of resistors from the same series increase with increasing sheet resistivities. The ratio between GFl and GFt varies

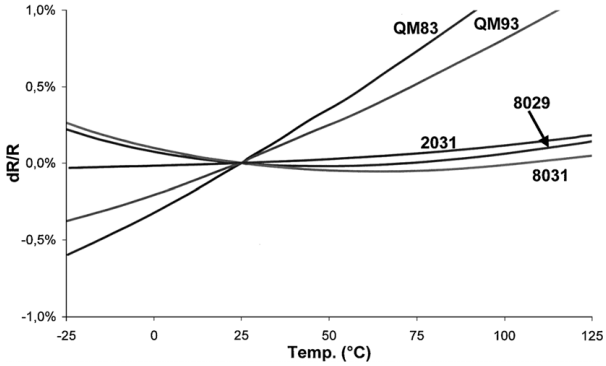

(a)

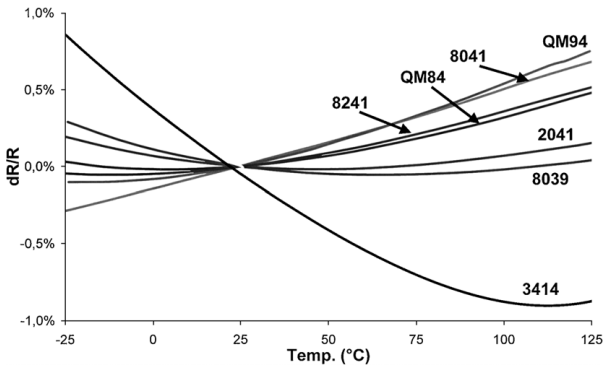

(b)

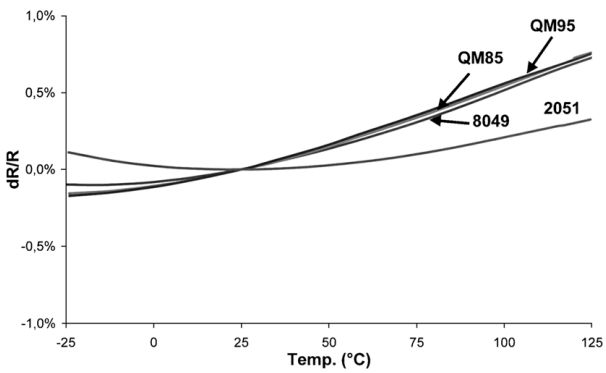

(c)

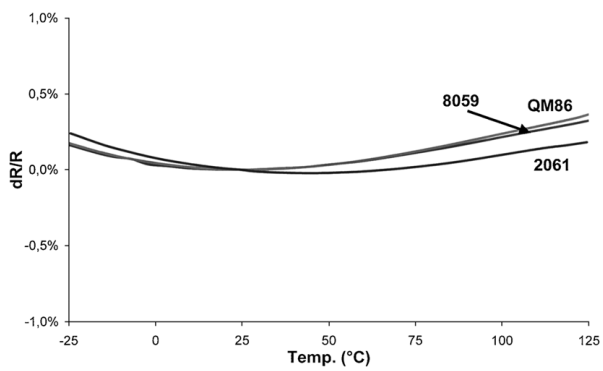

(d)

Figure 4 (a) The dependence of relative resistivity vs. temperature for 1 kohm/sq. thick film resistors; (b) The dependence of relative resistivity vs. temperature for 10 kohm/sq. thick film resistors; (c) The dependence of relative resistivity vs. temperature for 100 kohm/sq. thick film resistors; (d) The dependence of relative resistivity vs. temperature for 1 Mohm/sq. thick film resistors.

from around 70% to over 90%. Resistors from the RuO_2-based series HS-80 × 1 have lower gauge factors than these from the $Bi_2Ru_2O_7$-based 80 × 9 series. The highest GF_l was measured for resistors made with

TABLE III Longitudinal gauge factors (GF_l), transverse gauge factors (GF_t) and the ratio GF_t/GF_l of thick film resistors

Resistor	Nominal sheet resistivity (ohm/sq.)	GF_l	GF_t	Ratio GF_t/GF_l (%)
8029	1 k	10.5	7.5	75%
8031	1 k	2.5	2.0	80
2031	1 k	7.5	5.5	75
QM-83	1 k	4.5	3.5	79
QM-93	1 k	4.0	3.0	79
8039	10 k	12.5	10.5	84
8041	10 k	4.0	3.5	86
2041	10 k	12.0	9.5	78
QM-84	10 k	11.0	9.0	83
QM-94	10 k	10.0	8.0	78
3414 (ESL)	10 k	20.0	13	65
8241 (Her.)	10 k	16.5	13.5	81
8049	100 k	14.5	13.0	88
2051	100 k	135	10.5	80
QM-85	100 k	13.5	12.5	94
QM-95	100 k	13.0	12.0	92
8059	1 M	14.5	13.0	90
2061	1 M	14.5	13.0	90
QM-86	1 M	15.5	13.5	87

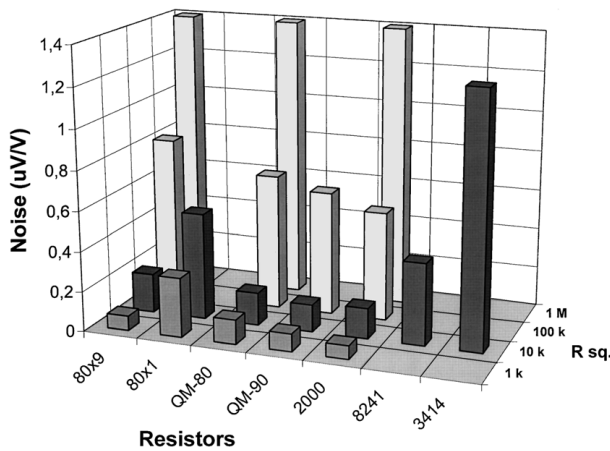

Figure 5 Noise indices of thick film resistors.

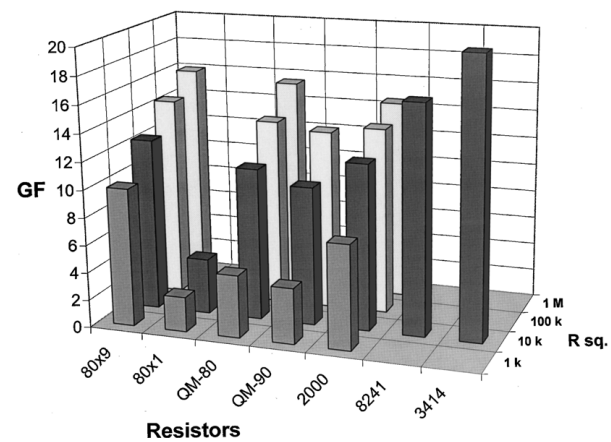

Figure 6 Longitudinal gauge factors of thick film resistors.

10 kohm/sq. ESL 3414 paste, which was developed by Electro Science Labs. to be used for strain gauge applications.

In the following few paragraphs it will be shown, at least tentatively, that the different chemical composition of the conductive phase in thick film resistors

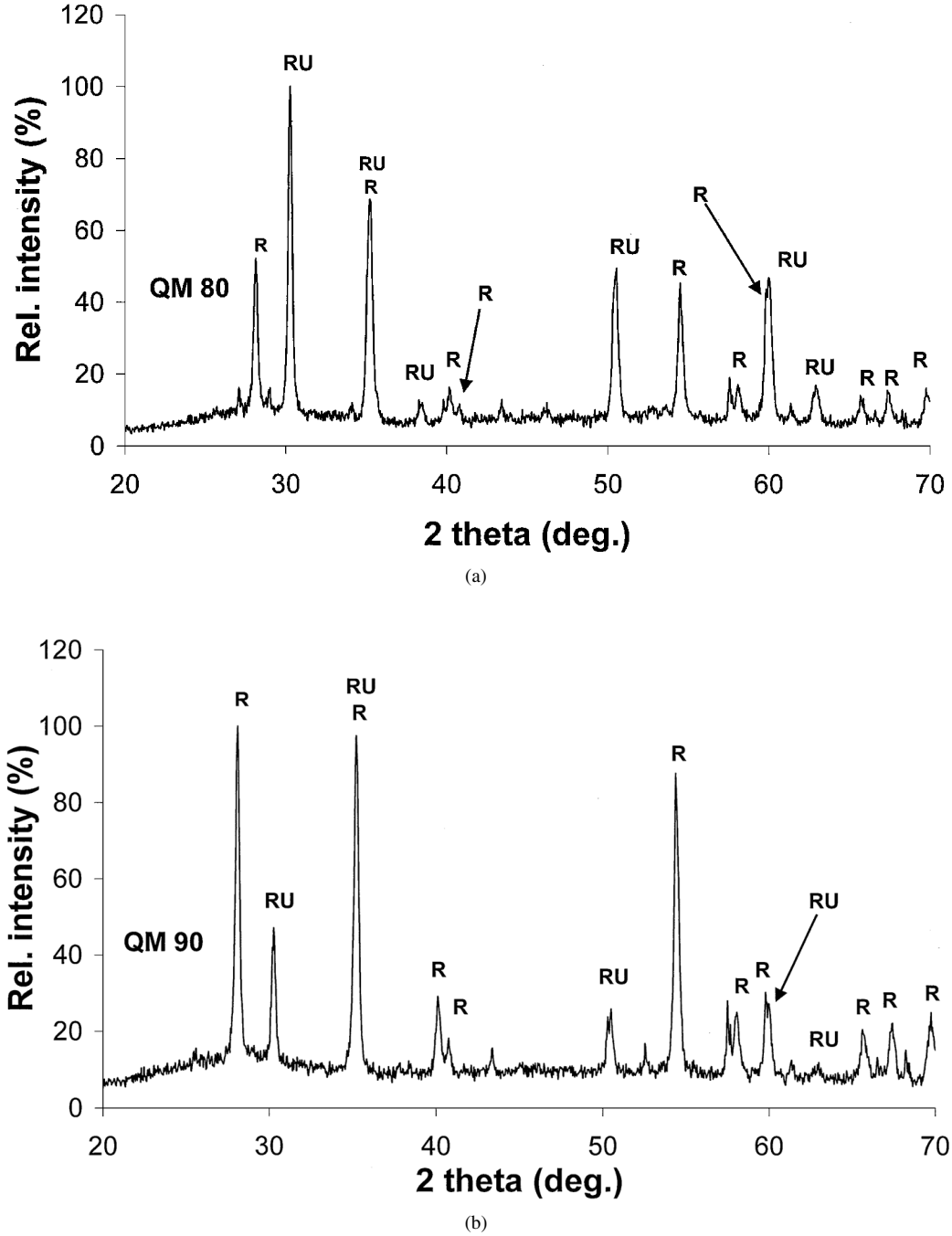

Figure 7 (a) X-ray spectra of the resistor QM-83 fired for 10 min at 850°C. RuO_2 peaks are denoted R and ruthenate peaks are denoted RU. (b) X-ray spectra of the resistor QM-93 fired for 10 min at 850°C. RuO_2 peaks are denoted R and ruthenate peaks are denoted RU.

is not the primary reason for the different gauge factors. For instance both the QM-80 and QM-90 series are based on a mixture of RuO_2 and ruthenate. X-ray spectra of the resistors QM-83 and QM-93 are shown in Fig. 7a and b, respectively. RuO_2 peaks aredenoted R and ruthenate peaks are denoted RU.

As mentioned in the Introduction, EDS quantitative analysis showed the presence of bismuth in the conductive phase which indicated that the ruthenate in these resistors is $Bi_2Ru_2O_7$. However, the calculated cell dimensions of the unit cell ($a = 1.021(1)$ nm) are smaller than the cell parameters of the cubic $Bi_2Ru_2O_7$ reported in the literature ($a = 1.0299$ nm) [18, 19]. Morten *et al*. observed a similar, but smaller, decrease of the $Bi_2Ru_2O_7$ unit cell dimensions in the pyrochlore based thick-film resistors after firing [20]. They attributed it to the partial exchange of bismuth ions in the pyrochlore structure with lead ions from the glass phase.

The relative intensities of the X-ray peaks of QM-80 and QM-90 resistor series show significantly different ratios of RuO_2 and ruthenate phases. QM 83 contains considerably more ruthenate than RuO_2 while the main conductive phase in QM 93 is RuO_2. However, as seen in Fig. 6, resistors from the QM-80 and QM-90 series with the same nominal sheet resistivity have nearly the same gauge factors. Microstructures of QM 83 and QM 93 are shown in Fig. 8a and b, respectively. The microstructures are rather similar; a mixture of a lighter conductive phase and a darker grey glass phase.

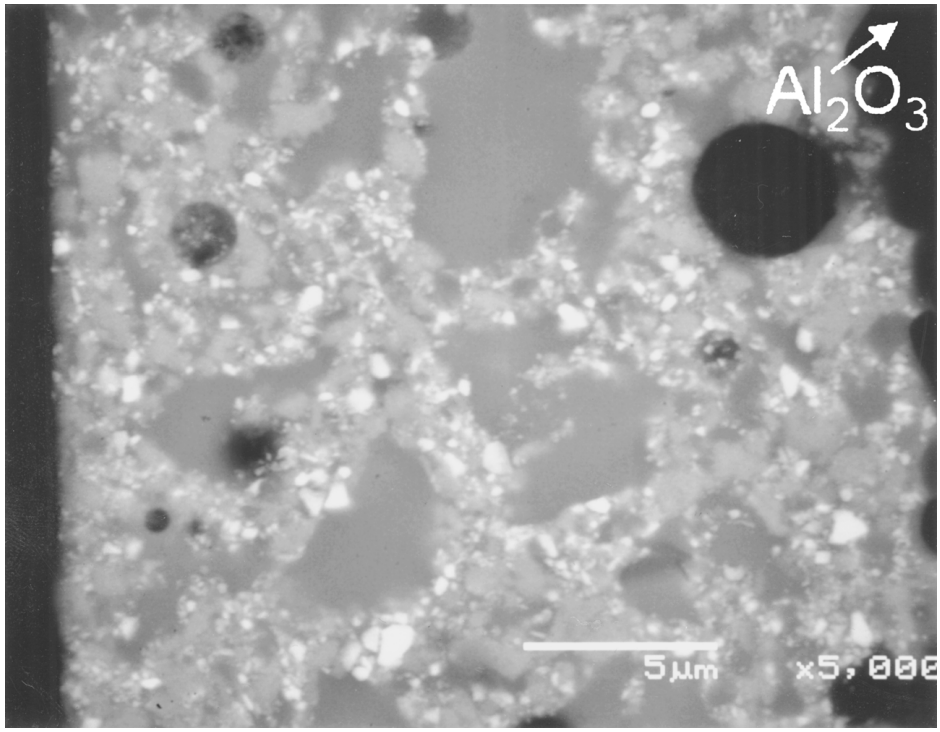

(a)

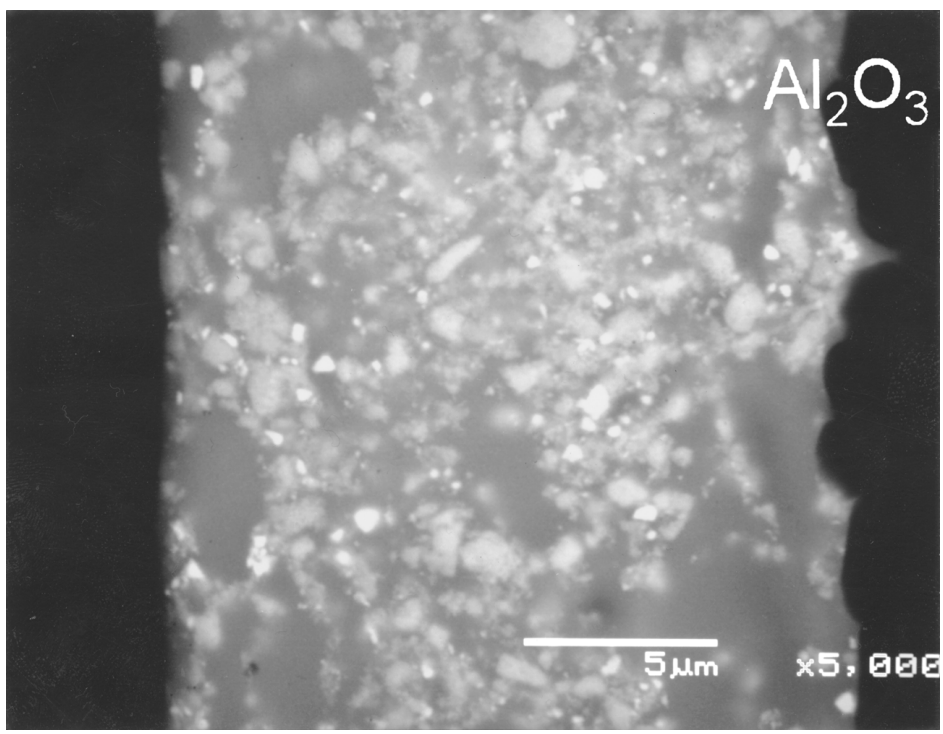

(b)

Figure 8 (a) Microstructure of a cross-section of the thick film resistor QM 83, fired for 10 min at 850°C. Alumina substrate is on the right. (b) Microstructure of a cross-section of the thick film resistor QM 93, fired for 10 min at 850°C. Alumina substrate is on the right.

Another example is the comparison of the 80×1 and 8241 resistors. The GF_l of the 80×1 resistors is below 4 while the GF_l of the 8241 is over 16. However, both are based on "pure" RuO_2 [11]. Microstructures of 8031 and 8241 are shown at different magnifications in Fig. 9a and b, and 10b and c, respectively. The alumina substrate is on the right. The microstructure of 8031 consists of "chains" of lighter phase conductive clusters (very small RuO_2 particles embedded in glass)—see Fig. 9b—around glass "islands", while 8241 is a mixture of lighter particles with sub-micrometer diameters of RuO_2 in a grey glass phase. These microstructures correspond to two different types of thick film resistor microstructures, described in the literature [21, 22]. The first type is characterised by the segregation of very small conductive particles in "chains" around larger

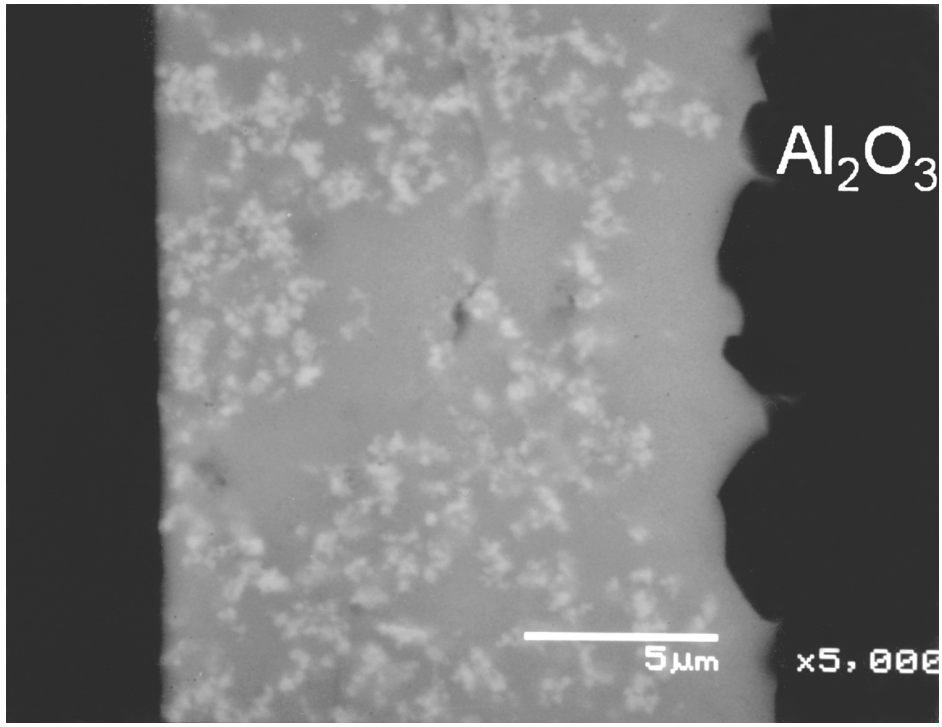

(a)

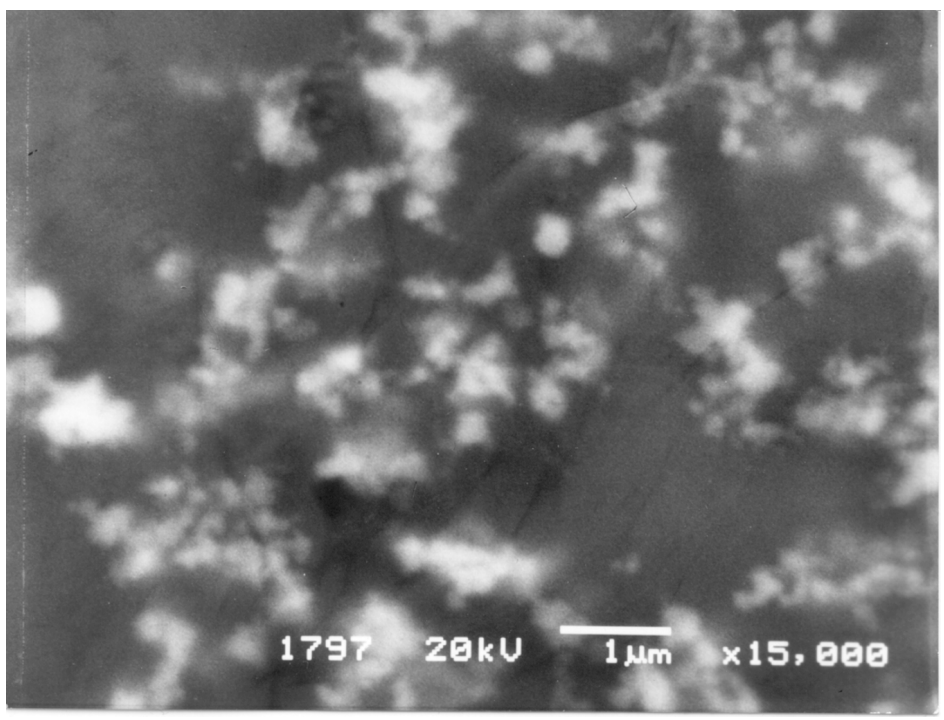

(b)

Figure 9 (a) Microstructure of a cross-section of the thick film resistor 8031, fired for 10 min at 850°C. Alumina substrate is on the right. (b) Microstructure of a cross-section of the thick film resistor 8031, fired for 10 min at 850°C (higher magnification).

sintered glass grains. The second type is a more or less homogenous mixture of conductive and glass phase.

The microstructure of 3414 resistor with the gauge factor even higher than that of 8241 is shown in Fig. 11. It consists of rather large light grains of ruthenate in glass matrix. The EDS quantitative microanalysis showed that the phase is mixed bismuth/lead ruthenate with the estimated formula of $(Bi_{0.5}Pb_{0.5})RuO_{7-x}$. This was confirmed by EDX analysis. The calculated cell dimensions of the unit cell ($a = 1.028(5)$ nm) are smaller than the cell parameters of the cubic $Bi_2Ru_2O_7$, as mentioned above about QM.80 and QM-90 resistor series. The microstructures of 3414 and 8241 are quite similar. However, the conductive phase in the 3414 is based on ruthenate and that in the 8241 is based on RuO_2.

These examples indicate that the microstructure of thick film resistors influences the gauge factors much more significantly than the "nature" of the conductive phase.

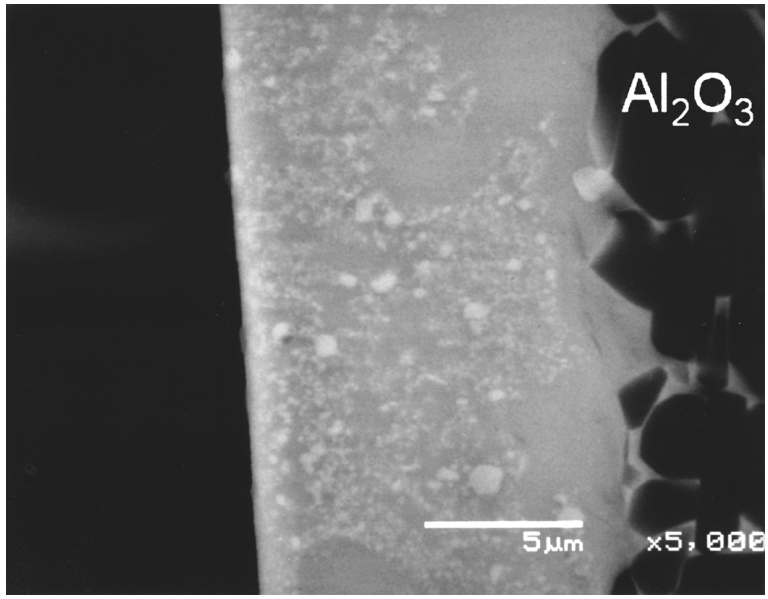

(a)

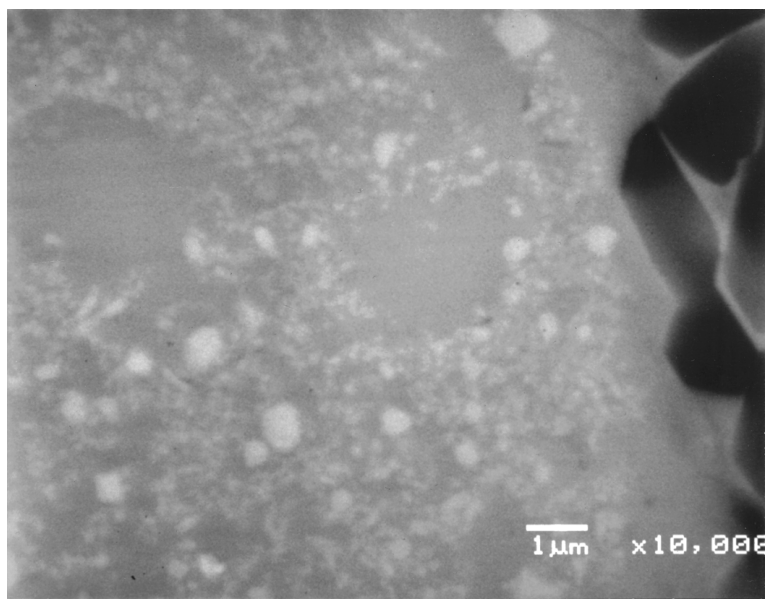

(b)

Figure 10 (a) Microstructure of a cross-section of the thick film resistor 8241, fired for 10 min at 850°C. Alumina substrate is on the right. (b) Microstructure of a cross-section of the thick film resistor 8241, fired for 10 min at 850°C (higher magnification). Alumina substrate is on the right.

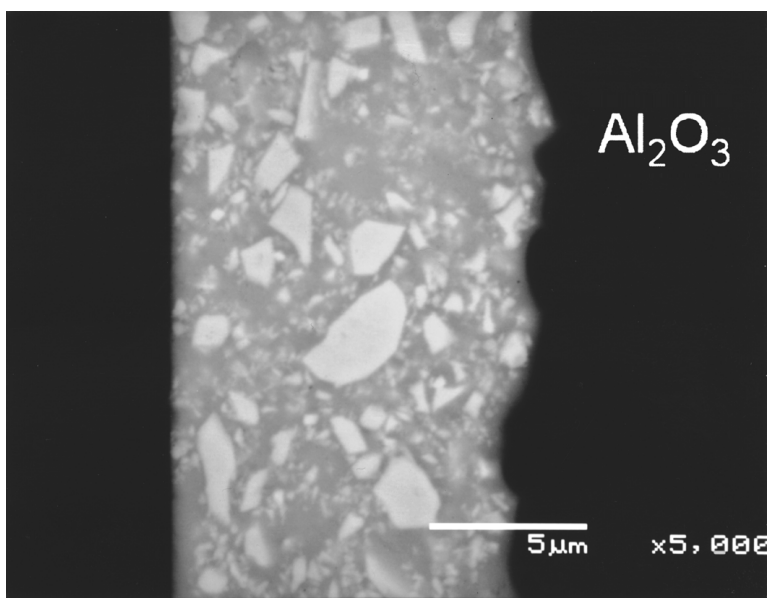

Figure 11 Microstructure of a cross-section of the thick film resistor 3414, fired for 10 min at 850°C. Alumina substrate is on the right.

4. Conclusions

Some commercial thick film resistors (Du Pont HS-80, QM-80, QM-90 and 2000, Electro Science Labs. 3414 and Heraeus 8241) with sheet resistivities from 1 kohm/sq. to 1 Mohm/sq. were evaluated for strain gauge applications. Temperature coefficients of resistivity, noise indices and gauge factors (GFs) were measured. The TCRs of most resistors are under 100×10^{-6}/K. Noise indices, longitudinal gauge factors (GF_l) and transverse gauge factors (GF_t) of resistors from the same series increase with increasing sheet resistivity. The ratio between GF_l and GF_t differs from around 70% to over 90%. The ESL 3414 resistors (10 kohm/sq) have the highest GF_l, around 20, but also the highest noise of +2 dB. It was shown, by comparing the chemical composition of the conductive phase, microstructures and GFs of different resistor series, that the different chemical composition of the conductive phase in thick film resistors is not the primary reason for the different values of gauge factors.

Acknowledgement

The authors wish to thank Mr. Mitja Jerlah (HIPOT) for printing and firing the samples as well as for the TCR, noise and gauge factors measurements, and Mrs. Jena Cilenšek (Jožef Stefan Institute) for the preparations of samples for SEM and EDS analysis. The financial support of the Ministry of Science and Technology of Slovenia is gratefully acknowledged.

References

1. K. HOFFMAN, "An Introduction to Measurements Using Strain Gauges" (Hottinger Baldwin Messtechnik GmbH, Darmstadt, 1989).
2. N. WHITE and A. CRANNY, *Hybrid Circuits* **12** (1987) 32.
3. O. ABE and Y. TAKETA, in Proc. 1988 Int. Symp. on Microelectronics ISHM-88, Seattle, 1988, 217.
4. M. PRUDENZIATI, B. MORTEN, F. CILLONI and G. RUFFI, *Sensors Actuators* **19** (1989) 401.
5. A. CATTANEO, R. DELL, ACQUA, G. DELL, ORTO, L. PIROZZI and C. CANALI, in Proc. 1980 Int. Symp. on Microelectronics ISHM-80, New York, 1980, p. 221.
6. A. G. BISHAY, D. A. ABDELHADY and A. M. DARWISH, *J. Mater. Sci.; Materials in Electronics* **3**(3) (1992) 195.
7. S. SATOH, Y. TAKATSUJI, F. KATOH and H. HIRATA, in Proc. 1991 Int. Symp. on Microelectronics ISHM-91, Orlando, 1991, p. 148.
8. N. M. WHITE and J. D. TURNER, *Meas. Sci. Technol.* **8**(1) (1997) 1.
9. C. CANALI, D. MALAVASI, B. MORTEN, M. PRUDENZIATI and A. TARONI, *J. Appl. Phys.* **51**(6) (1980) 3282.
10. M. PRUDENZIATI and B. MORTEN, *Hybrid Circuits* **10**(20) (1986) 37.
11. M. HROVAT, G. DRAŽIČ, J. HOLC and D. BELAVIČ, *J. Mater. Sci. Lett.* **14**(15) (1995) 1048.
12. M. HROVAT, D. BELAVIČ, J. HOLC and S. ŠOBA, *ibid.* **13** (1994) 992.
13. M. HROVAT, J. HOLC, Z. SAMARDŽIJA and D. BELAVIČ, in Proc. 22nd Int. Spring Seminar on Electronics Technology ISSE 99, edited by W. Sauer and K. J. Wolter (Freital-Dresden, 1999) p. 328.
14. M. HROVAT, Z. SAMARDŽIJA, J. HOLC and D. BELAVIC, *J. Mater. Sci.; Materials in Electronics* **11**(3) (2000) 199.
15. S. CHITALE, C. HUANG and M. STEIN, *Hybrid Circuits Technol.* **6**(5) (1989).
16. C. SONG, D. V. KERNS, JR., J. L. DAVIDSON, W. KANG and S. KERNS, in IEEE Proc. SoutheastCon 91 Conf., Williamsburg, 1991, Vol. 2 p. 1106.
17. K. ADACHI and H. KUNO, *J. Amer. Ceram. Soc.* **80**(5) (1997) 1055.
18. R. J. BOUCHARD and L. J. GILLSON, *Mater. Res. Bull.* **6**(8) (1971) 669.
19. M. A. SUBRAMANIAN, G. ARAVAMUDAN and G. V. S. RAO, *Progress in Solid State Chem.* **24** (1981) 55.
20. B. MORTEN, A. MASOERO, M. PRUDENZIATI and T. MANFREDINI, *J. Phys. D: Appl. Phys.* **27**(10) (1994) 2227.
21. T. V. NORDSTROM and C. R. HILLS, in Proc. Int. Hybrid Microelectronics Symp. ISHM-79, Los Angeles, 1979, p. 40.
22. A. KUBOVY, *J. Phys. D: Appl. Phys.* **19** (1986) 2127.

Received 10 May
and accepted 15 November 2000